the tube was found to be about 51.0 kips. The attachment area suffered no discernible damage.

VII. Conclusions

The following conclusions may be made: 1) design parameters can be optimized conveniently by the structural synthesis approach in determining the minimum weight configuration, and 2) the shim-joint concept can be successfully applied to composite members without prohibitive attachment weight penalties.

References

[1] Cole, B. W., Wong, J. P., and Courtney, A. L., "Development of the Shim Joint Concept for Structural Members," Tech. Rept. AFFDL-TR-67-116, Aug. 1967, Air Force Flight Dynamics Lab., Wright-Patterson Air Force Base, Ohio.

[2] "Exploratory Application of Filament Wound Reinforced Plastic for Aircraft Landing Gear," Tech. Rept. AFML-TR-66-309, Dec. 1966, The Bendix Corp., Products Aerospace Div.

[3] "Large Segmented Fiber Glass Reinforced Plastic Rocket Motor Cases," Rept. ASD-IR-8-150, Vol. I–VIII, Thiokol Chemical Corp., Wasatch Div.

[4] Goland, M. and Reissner, E., "The Joint Stresses in Cemented Joints," *Journal of Applied Mechanics*, Vol. 11, March 1944, pp. A17–A27.

[5] Melcon, M. A. and Hoblit, F. M., "Analysis of Lugs and Shear Pins," *Product Engineering*, May 1950, p. 113, and June 1953, p. 160.

[6] "Mechanics of Adhesive Bonded Lap-Type Joints: Survey and Review," Rept. ML-TDR-64-298, 1964, Forest Product Lab., U.S. Dept. of Agriculture, Madison, Wis.

[7] "Manufacturing Methods for Plastic Airframe Structures by Filament Winding," Tech. Rept. IR-9-371(1), Feb. 1967, Air Force Materials Lab., Wright-Patterson Air Force Base, Ohio.

[8] Ridha, R. A. and Wright, R. N., "Minimum Cost Design of Frames," *Journal of Structural Division, Proceedings of the American Society of Civil Engineers*, Vol. 93, ST4, Aug. 1967, Paper 5394.

JAN.-FEB. 1969 J. AIRCRAFT VOL. 6, NO. 1

Damping of High-Frequency Brake Vibrations in Aircraft Landing Gear

A. K. Abu-Akeel*
The Bendix Corporation, South Bend, Ind.

This paper outlines the nature of high-frequency brake-excited vibrations and shows how a tuned damper can effectively suppress the excitation. The problem, defined as a self-excited, two-mass system, is analyzed and a closed-form solution is obtained. An energy balance approach is utilized to treat the possible nonlinear functions present in the system. It is shown that the two resulting modes are stable within a defined range of frequency ratio and secondary system damping. This range is affected by the mass ratio and the intensity of excitation, i.e., negative damping. Stability charts are plotted to help select the optimum size, tuning, and damping conditions of a brake-tuned damper effective under actual service conditions. Experimental results are shown to confirm the theoretical analysis.

Nomenclature

C_1, C_2 = equivalent viscous damping constants of the primary and secondary systems respectively, lb sec/in.
E = energy, lb in.; subscripts i, d, and v refer to input, damped, and viscous damping energy, respectively
f_1, f_2 = primary system and secondary system (damper) positive damping functions, respectively
I_1, I_2 = total polar moment of inertia of the primary and secondary systems, respectively in. lb sec^2
K_1, K_2 = equivalent stiffness of the primary and secondary system springs, respectively, in. lb/rad
M = margin of stability; subscripts v and h for viscous and hydrodynamic damping, respectively
n_i = damping parameters of the two modes of motion, $i = 1,2$
p_i = frequency parameters of the two modes of motion, $i = 1,2$
r_i = frequency ratio, $r_i = p_i/\omega_2$, $i = 1,2$
T = torque applied to the brake, in. lb
x = frequency ratio ω_2/ω_1, a wear parameter
$x_{\min}, x_{\max}$ = limiting values of x, beyond which either or both modes are unstable
θ_{ij} = amplitude of system j,($j = 1,2$) in mode i, $i = 1,2$
θ_1, θ_2 = angular deflection of fixed parts of the brake (primary system) and of the secondary system, respectively, rad
η_i = damping parameter = n_i/ω_2, $i = 1,2$
μ = I_2/I_1, mass ratio
ω_1, ω_2 = natural frequency of primary system, $(K_1/I_1)^{1/2}$ and of secondary system, (K_2/I_2),$^{1/2}$ respectively, rad/sec
ζ_1 = primary system negative damping factor = $C_1/2I_1\omega_1$
ζ_2 = secondary system positive damping factor = $C_2/2I_2\omega_2$

Presented as Paper 68-312 at the AIAA/ASME 9th Structures, Structural Dynamics, and Materials Conference, Palm Springs, Calif., April 1–3, 1968; submitted March 25, 1968; revision received July 1, 1968.

* Analytical Specialist, Energy Controls Division.

I. Introduction

VIBRATIONS induced by brakes in landing gears have become a sizeable problem for brake manufacturers since harder cermetallic linings were introduced. The excellent wear characteristics of those linings are associated with increased braking roughness, i.e., excessive vibrations.

The three modes of vibrations usually observed during brake application, are described as follows: 1) chatter mode, involves back-and-forth oscillations (fore and aft) of the

carriage at a frequency in the order of 8–15 cps; 2) the primary squeal mode, high-frequency torsional oscillations in the order of 200–300 cps, in which the stationary parts of the brake and the mounting axle form a torsional system; 3) secondary squeal mode, of a much higher frequency, in the order of 1000–2000 cps, acts as a multidegree-of-freedom system within the brake assembly itself. Still higher modes could be excited but are usually of negligible energy capacities.

The primary squeal and the chatter modes are the most pronounced. They were reported to be responsible for passenger discomfort, chatter of instrumentations, considerable noise, and sometimes for fatigue failure of some brake components. The nature of brake excitation is only partially understood. However, the fact that torque variation with speed, during braking torque curve slope, is responsible for brake excitation is well known. This is equivalent to a variation of the coefficient of friction with the relative slip velocity, hence negative damping, for a negative torque curve slope. R. Black[1] has shown that torque irregularities can be responsible for squeal and chatter excitation and their limit cycle, and sometimes coupling between the two modes.

Some factors affecting the brake response to any form of excitation attributable to the lining characteristics are 1) surface and/or bulk temperature of the brake, 2) slip velocity, 3) normal pressure, 4) brake structural damping, 5) construction geometry, and 6) stick-slip conditions. The temperature of the lining surface can be expected to affect the excitation, whereas the bulk/brake temperature may affect the amount of positive damping present and, hence, the brake response.

Current approaches attempt to increase the damping capability of the structural parts within the brake torque path. These include modified rotor and stator configuration, in-line dampers (e.g., friction and viscoelastic couplings, etc.), and friction joints.

Because of their rough behavior in the brake, the hard linings were usually discarded despite their good wearing qualities. Therefore, it was necessary to develop dampers for application to brake vibrations in the hope that harder linings may then be utilized. This could mean considerably longer lining life, lighter brakes, and sizeable savings.

In order to separate the damper application study from the basic problem of brake excitation without going into a number of doubtful assumptions, the effect of excitation will be lumped into a single coefficient based on energy balance. The same is done to the over-all effect of all factors influencing the amount of positive damping in the system, as will be shown in Sec. II.

Although some coupling may exist between the two basic modes, chatter and squeal, the problem of applying a damper to the brake can be greatly simplified if the two modes were decoupled. Considering each mode separately does not introduce too much error since the two frequencies are widely separated and the damper is expected to tune closely to the squeal mode frequency, and hence may not affect the chatter mode. The brake-damper assembly can then be treated as a two-degree-of-freedom torsional system. The excitation can be approximated by a negative damping coefficient yielding the same energy input which may be dependent upon the amplitude. Section III is concerned with the analytical solution of this problem.

In Sec. IV, the stability of the system is discussed to show the design limits on the tuning of the damper. This applies to its frequency, size, and internal damping conditions.

Section V describes the stability charts in general and the effects of the different parameters of the system on their characteristics. In Sec. VI, the application of stability charts to a hydraulically damped (velocity square damping) secondary system is discussed. The results of an experimental application are given in Sec. VII and show how well the theory can lead to the design of an effective brake damper.

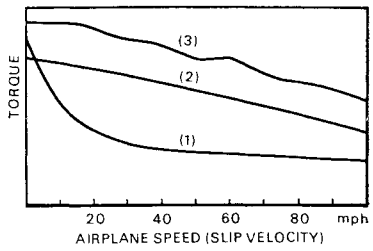

Fig. 1 Samples of torque function plots. (1) Excessive torque build-up at low speeds, uniform torque at high speeds, highest vibration level at low speeds, moderately rough. (2) Continuous torque build-up during braking, vibration starts at high speeds and has longer build-up period, very rough. (3) Same as (2) but with excessive irregularities, excessive chatter.

Although this study is oriented primarily towards the problem of applying a tuned damper to a torsional brake system, the same basic analysis applies to any self-excited, two-mass system and may be utilized, for example, in the study of vibration of machine tools.

II. Torque and Damping Functions

Torque Function

The brake torque may be expressed as a function of the slip velocity, i.e., the relative velocity between the brake rotors and stators. The friction characteristics of the lining determine the form of the torque function. Figure 1 shows some typical torque functions for different linings.

Within any stop interval, the torque may be expressed by a function of the form

$$T = T(\dot{\theta}_1, \omega_t) \tag{1}$$

determined from the torque function plot of the lining after its characteristics had stabilized, ω_t is the angular velocity of the rotors, and $\dot{\theta}_1$ is the angular velocity of stators. The rate of energy input/cycle, E_i, in the brake-damper system due to this torque function is given by

$$E_i = \int_0^{2\pi} T d\theta_1$$

where θ_1 = angular deflection of the fixed parts of the brake. The study of E_i for different linings and factors affecting the torque function is a different subject which will not be treated here. The torque function plot is usually available. An equivalent negative viscous damping coefficient C_1 will be derived and inserted in the equation of motion to yield the same energy input/cycle E_i. This coefficient is amplitude dependent and hence preserves the nonlinear character of the system without complicating the analysis. This is done as follows.

Energy input due to a negative viscous damping coefficient C_1,

$$E_v = \int_0^{2\pi} C_1 \dot{\theta}_1 d\theta_1 = \pi C_1 \omega_1 \theta_0^2 \tag{2}$$

for a mode exercising simple harmonic motion, where ω_1 = frequency of vibration and θ_0 = angular amplitude.

E_v must be equivalent to the energy input/cycle due to the torque function less the energy damped within the brake structure E_d, i.e., $E_v = E_i - E_d$. Therefore,

$$\pi C_1 \omega \theta_0^2 = E_i - E_d$$

and

$$C_1 = (E_i - E_d)/\pi \omega_1 \theta_0^2 \tag{3}$$

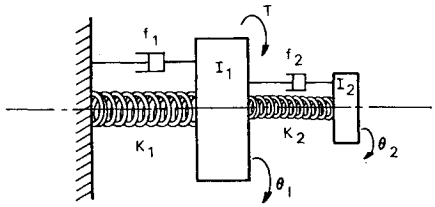

Fig. 2 Two-mass torsional system.

Brake Damping Function

It is not feasible to assume any particular damping function within the brake and apply it to the equations of motion of the system. Damping may be caused by a number of related or nonrelated factors, e.g., dry friction, hysteretic damping due to elastic and plastic deformation of brake elements, . . . etc. The over-all damping effect may be represented by some nonlinear function $f_1(\theta_1,\dot{\theta}_1)$. Although the form of this function may never be established, its over-all effect is a dissipation of part E_d, of the energy input E_i and a reduction of the net negative damping coefficient C_1 as given by Eq. (3).

The net result C_1 may thus be obtained from a study of the torque function and an assumption of an equivalent damping coefficient to yield the same energy dissipation E_d, or from a study of the free vibration response of the brake.

Damper Damping Function

Most tuned dampers are fitted with viscous damping means. For brake vibration, hydraulic damping seems very promising. Because the brake vibrations are self-excited, they need little damping at low amplitudes, but high damping at higher amplitudes if vibration is to be kept at a minimum level. This is best supplied by hydraulic damping since its damping force is proportional to the square of the relative velocity rather than the velocity itself as for viscous damping. Whichever damping function is used, an equivalent viscous coefficient C_2 may be derived to yield the same energy dissipation per cycle of the damper relative oscillation. If f_2 is the damping force, the energy dissipated per cycle due to f_2 must be equal to the energy dissipated due to C_2, i.e.,

$$\int_0^{2\pi} f_2 \frac{(\dot{\theta}_1 - \dot{\theta}_2)}{|\dot{\theta}_1 - \dot{\theta}_2|}\, d(\theta_1 - \theta_2) = \pi\omega(\theta_1 - \theta_2)_0{}^2 C_2$$

or

$$C_2 = \frac{1}{\pi\omega(\theta_1 - \theta_2)_0{}^2} \int^{2\pi} f_2 \frac{(\dot{\theta}_1 - \dot{\theta}_2)}{|\dot{\theta}_1 - \dot{\theta}_2|}\, d(\theta_1 - \theta_2) \tag{4}$$

where, the subscript 0 refers to the amplitude of oscillation.

The condition of hydraulic damping is given by

$$f_2 = C_h(\dot{\theta}_1 - \dot{\theta}_2)^2 \tag{5}$$

where C_h = hydraulic coefficient. In this case,

$$C_2 = (8\omega/3\pi)(\theta_1 - \theta_2)_0 C_h \tag{6}$$

The dependence of C_2 on $(\theta_1 - \theta_2)$ preserves the nonlinear nature of the hydraulic damping.

It should be noted that the damping function f_2 may be a combination of viscous, hydraulic, and dry friction damping effects. In such case, the energy balance approach will help sum up all the effects in a simple equivalent coefficient.

III. Solution to the Problem of a Two-Degree-of-Freedom System Acted Upon by Friction Excitation

This problem represents the squeal system of the brake when fitted with a single damper of the tuned type. The system is illustrated in Fig. 2.

The equation of motion can be written as

$$I_1\ddot{\theta}_1 + f_1(\theta,\dot{\theta})\dot{\theta}_1 + K_1\theta_1 + f_2 \frac{(\dot{\theta}_1 - \dot{\theta}_2)}{|\dot{\theta}_1 - \dot{\theta}_2|} + K_2(\theta_1 - \theta_2) = T \tag{7a}$$

for the primary mass I_1 and

$$I_2\ddot{\theta}_2 + f_2 \frac{\dot{\theta}_2 - \dot{\theta}_1}{|\dot{\theta}_2 - \dot{\theta}_1|} - K_2(\theta_1 - \theta_2) = 0 \tag{7b}$$

for the secondary mass I_2, where T is given by Eq. (1).

The function $f_1(\theta,\dot{\theta})$ was discussed in Sec. II and was shown to be reducible to an equivalent viscous damping coefficient yielding the same energy dissipation per cycle. The function $f_2[(\theta_1 - \theta_2), (\dot{\theta}_1 - \dot{\theta}_2)]$ is the damping function within the tuned damper and depends on its design. Two forms may be applied and allowed for in its construction: 1) viscous damping $f_2 = C|\dot{\theta}_2 - \dot{\theta}_1|$; 2) hydraulic damping where f_2 is given by Eq. (5). Expressions involving dry friction or hysteretic damping may also be proposed. Viscoelastic damping materials require another different form.

The solution, based on energy consideration, reduces the complex damping function form to a constant damping coefficient C_2 representing an equivalent viscous damping effect. Although a time solution may be in error, the over-all picture of the two primary harmonic modes can be closely approximated. No other harmonics, however, have been observed in practice and the solution can then be applied. It was also shown that the input function T can be substituted by an equivalent negative damping coefficient of viscous nature to yield the same input energy to the motion of the primary system, i.e., the brake.

In essence, Eqs. (7) can be reduced to Eqs. (8):

$$I_1\ddot{\theta}_1 - (C_1 - C_2)\dot{\theta}_1 + K_1\theta_1 - C_2\dot{\theta}_2 + K_2(\theta_1 - \theta_2) = 0 \tag{8a}$$

$$I_2\ddot{\theta}_2 + C_2(\dot{\theta}_2 - \dot{\theta}_1) + K_2(\theta_2 - \theta_1) = 0 \tag{8b}$$

This is the problem of transient oscillations of a damped two-degree-of-freedom system. A solution will be obtained and stability of the system examined. Equations (8) represent two second-order linear differential equations for which a solution can be obtained if we let

$$\theta_1 = Ae^{St} \qquad \theta_2 = Be^{St} \tag{9}$$

This solution yields the following characteristic equation:

$$S^4 + A_3S^3 + A_2S^2 + A_1S + A_0 = 0 \tag{10}$$

This fourth-order algebraic equation has, in general, four roots. For a harmonic solution, the roots will be of complex form and occur in conjugate pairs. Assume for a solution

$$S_{1,2} = n_1 \pm ip_1 \qquad \text{and} \qquad S_{3,4} = n_2 \pm ip_2 \tag{11}$$

where $i = (-1)^{1/2}$. Equation (10) can then be put in the form

$$(S - S_1)(S - S_2)(S - S_3)(S - S_4) = 0 \tag{12}$$

Substituting for S_1, S_2, S_3, and S_4 from Eq. (11) into Eq. (12) and performing a direct analogy to Eq. (10), we obtain

$$A_3 = a_1(1 + \mu) + a_2 = -2(n_1 + n_2) \tag{13a}$$

$$A_2 = \omega_1{}^2 + \omega_2{}^2 + a_1a_2 + \mu\omega_1{}^2 = |S_1|^2 + |S_3|^2 + 4n_1n_2 \tag{13b}$$

$$A_1 = \omega_2{}^2a_2 + \omega_1{}^2a_1 = -2(n_2|S_1|^2 + n_1|S_2|^2) \tag{13c}$$

$$A_0 = \omega_1{}^2 \cdot \omega_2{}^2 = |S_1|^2 \cdot |S_2|^2 \tag{13d}$$

where $a_1 = C_2/I_2$, $a_2 = -C_1/I_1$, and ω_1,ω_2 and μ are defined in the Nomenclature.

Although no approximation is necessary to obtain a solution along the boundaries of the domain of stability, where $n_i \leq 0$, $i = 1$ or 2, a more general solution, valid within the domain of stability, can be obtained assuming that $n_1{}^2 \ll$

p_i^2; in this case

$$|S_i|^2 = n_i^2 + p_i^2 \sim p_i^2 \qquad i = 1,2$$

For example, $n_1 = 0$, on the boundary of the stability loop of Fig. 3, and $n_2^2 = 0.005\ p_2^2$ at $x = 0.9$ as is given by Eq. (13a). Within the stability domain $n_i \neq 0$ but the ratio $(n_i/p_i)^2$ is still of the same order of magnitude. It is therefore justified to assume that small damping conditions prevail and $n_i^2 \ll p_i^2$.

From Eqs. (13b) and (13d) we obtain the following frequency equation:

$$p^4 - [\omega_1^2(1 + \mu) + \omega_2^2 + a_1a_2]p^2 + \omega_1^2\omega_2^2 = 0 \quad (14)$$

which has the roots

$$p_{1,2}^2 = \frac{1}{2}[\omega_1^2(1 + \mu) + \omega_2^2 + a_1a_2 \pm \{[\omega_1^2(1 + \mu) + \omega_2^2 + a_1a_2]^2 - 4\omega_1^2\omega_2^2\}^{1/2}] \quad (15$$

and by choice let p_2 be the bigger root. Equations (13a) and (13c) yield the following expressions for n_1 and n_2:

$$n_1 = -\frac{a_1[\omega_1^2 - p_1^2(1 + \mu)] + a_2[\omega_2^2 - p_1^2]}{2(p_2^2 - p_1^2)}$$

$$n_2 = \frac{a_1[\omega_1^2 - p_2^2(1 + \mu)] + a_2[\omega_2^2 - p_2^2]}{2(p_2^2 - p_1^2)} \quad (16)$$

The solution (9) can then be written as

$$\theta_1 = \theta_{11}e^{n_1t}\sin(p_1t + \phi_1) + \theta_{12}e^{n_2t}\sin(p_2t + \phi_2) \quad (17a)$$

$$\theta_2 = \theta_{21}e^{n_1t}\sin(p_1t + \phi_1) + \theta_{22}e^{n_2t}\sin(p_2t + \phi_2) \quad (17b)$$

θ_{11}, θ_{12}, ϕ_1, and ϕ_2 are constants to be determined from the initial conditions. The ratios θ_{21}/θ_{11} and θ_{22}/θ_{12} can be obtained by substituting this solution into either of Eqs. (8).

Therefore,

$$\frac{\theta_{21}}{\theta_{11}} = \frac{2n_1I_1 + C_2 - C_1}{C_2} \qquad \frac{\theta_{22}}{\theta_{12}} = \frac{2n_2I_1 + C_2 - C_1}{C_2} \quad (18)$$

IV. Conditions of Stability

According to Eqs. (17) a mode i will be stable if $n_i \leq 0$ which upon substitution in Eq. (16) gives the following result:

$$\frac{\omega_2^2 - p_1^2}{p_1^2(1 + \mu) - \omega_1^2} \geq \frac{a_1}{a_2} \geq \frac{\omega_2^2 - p_2^2}{p_2^2(1 + \mu) - \omega_1^2} \quad (19)$$

where $p_2 > p_1$. The case when $p_1 = p_2$ is a special one which should be treated separately and for which a solution of the form $\theta = (a + bt)e^{st}$ may be assumed instead of expression (9).

Another limit is imposed on the system by the requirement that the motion of either mode be harmonic. This requires that both p_1 and p_2 be real. Equation (15) then dictates that

$$\omega_1^2(1 + \mu) + \omega_2^2 + a_1a_2 > +2\omega_1\omega_2 \quad (20)$$

Because we are interested in the behavior of the brake-damper system in actual service, the effect of wear on the mass of the primary system has to be investigated. All the parameters of the system will, therefore, be referred to the arbitrary condition when $\omega_1 = \omega_2$. A change in I_1 to I_1x^2, where the brake wear parameter x is a factor greater than 0, will result in the following changes: $(I_1)_x = I_1x^2$, $(\mu)_x = \mu/x^2$, and $(\omega_1)_x = \omega_1/x$ where the x subscript indicates the conditions at $x \neq 1$.

If we now introduce the following nondimensional factors referred to ω_2 rather than ω_1, which changes with brake wear:

$$r_1 = p_1/\omega_2 \qquad r_2 = p_2/\omega_2$$

$$\eta_1 = n_1/\omega_2 \qquad \eta_2 = n_2/\omega_2$$

$$\zeta_2 = C_2/2I_2\omega_2 = a_1/2\omega_2$$

$$\zeta_1 = C_1/2I_1\omega_1 = -a_2/2\omega_1$$

ζ_1 will also change to ζ_1/x, and inequalities (19) and (20) take the following convenient forms:

$$\frac{(r_1^2 - x^2)\zeta_1}{r_1^2(x^2 + \mu) - x^2} \leq \zeta_2 \leq \frac{(r_2^2 - x^2)\zeta_1}{r_2^2(x^2 + \mu) - x^2} \quad (21)$$

$$\zeta_2 < (1/4\zeta_1)[1 + (\mu/x^2) + x^2 - 2x] \quad (22)$$

where r_1 and r_2 are given by

$$r_1^2 = \frac{1}{2}\left[1 + \frac{\mu}{x^2} + x^2 - 4\zeta_1\zeta_2 - \left\{\left(1 + \frac{\mu}{x^2} + x^2 - 4\zeta_1\zeta_2\right)^2 - 4x^2\right\}^{1/2}\right] \quad (23)$$

and

$$r_2^2 = \frac{1}{2}\left[1 + \frac{\mu}{x^2} + x^2 - 4\zeta_1\zeta_2 + \left\{\left(1 + \frac{\mu}{x^2} + x^2 - 4\zeta_1\zeta_2\right)^2 + 4x^2\right\}^{1/2}\right] \quad (24)$$

The amplitude ratios of Eqs. (18) become

$$\theta_{2i}/\theta_{1i} = 1 + (x^2\eta_i - \zeta_1)/\mu\zeta_2 \quad (25)$$

which at neutral stability, $n_i = \eta_i = 0$, becomes

$$\theta_{2i}/\theta_{1i} = 1 - (\zeta_1/\mu\zeta_2) \quad (26)$$

for either mode. This is the magnification ratio or the ratio between the amplitude of the secondary system, damper mass, to that of the primary system, i.e., the brake; it helps define the amplitude of oscillation of the mass of the damper at any limit cycle amplitude attained by the brake.

Some other interesting results describing the interaction between the two system modes can be obtained[2]; however, they will not be derived here to concentrate on the more relevant material.

V. Stability Charts of a Self-Excited Two-Mass System

The results of Sec. IV give the conditions of stable or unstable operation of the self-excited two-mass system in terms of the following variables: 1) the ratio x between the natural frequencies of the coupled systems, 2) the mass ratio μ referred to the conditions at $x = 1$, 3) the amount of negative damping supplied to the primary system and given by the ratio ζ_1, 4) the amount of positive damping supplied to the relative motion between the two masses and referred to the secondary system by the ratio ζ_2. The stability charts are plots of the conditions of stability, inequalities (21) and (22), showing the interacting effects of the parameters x, μ, ζ_1, and ζ_2 on the stability of either or both modes. In Fig. 3,

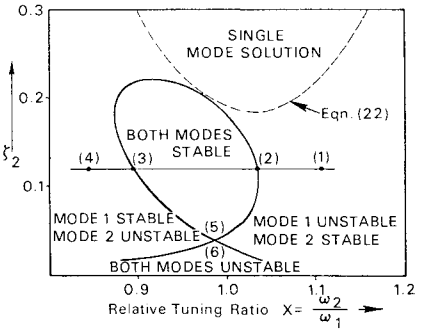

Fig. 3 Stability loops, $\mu = 0.03$, $\zeta_1 = 0.04$.

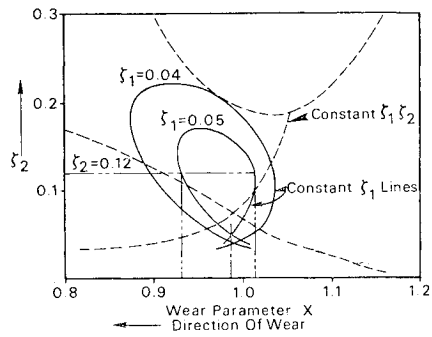

Fig. 4 Stability charts, ($\zeta_2 - x$ plots). Brake is stable, no squeal build-up, between $x = 1.01$ and $x = 0.93$ when $\zeta_1 = 0.05$, $\zeta_2 = 0.12$, and $\mu = 0.03$.

lines of constant values of ζ_1 form a closed loop in a $\zeta_2 - x$ plane; within the loop both modes will be stable, i.e., any excitation will be damped out and no oscillations are allowed to build up. Below the divergent terminals of the loop both modes exist and will be unstable. Above the line marked "Eq. (22)," the two-mode solution does not exist and only the primary system motion can be observed; this is the condition when the secondary system moves as a part of the primary mass. To the left and to the right of all the limiting lines of stability only one mode will be stable and the other one unstable.

The variation of the relative tuning x between the two primary frequencies of a given system affects the conditions of stability of either or both modes. Referring to Fig. 3 and the loop given by some constant value of ζ_1, if we start at point (1) mode 2 will be stable and mode 1 unstable. At point (2) mode 1 will reach neutral stability. Between points (2) and (3) both modes are stable. Point (3) represents the conditions when mode 2 reaches neutral stability while at point (4) mode 2 is unstable and mode 1 stable. At point (5) both modes are neutrally stable and at point (6) both are unstable.

In a brake-damper system the change in x may be due to wear in brake lining, which increases the brake natural frequency and, hence, decreases x since the damper frequency can be assumed unchanged. Throughout the life of the brake lining, the relative tuning ratio x should lie between points (2) and (3) of Fig. 3, located on the loop given by the proper value of ζ_1, which is a property of the lining itself (c.f., Sec. II). The distance between points (2) and (3) is defined as the margin of stability and depends on the value of ζ_2. The largest margin of stability is designated M_v and corresponds to the optimum value of ζ_2 at which a viscously damped absorber (damper) may be designed. Increasing the mass ratio μ will expand the stability loops and thus help finding a proper damper size for any required change in M_v. Increasing the amount of negative damping ζ_1 in the system reduces the optimum margin of stability by resulting in smaller loops (Fig. 4). From those two opposite effects of μ and ζ_1 it can then be concluded that: "A damper of a given size may be fitted to a small system (larger μ) of high negative damping (larger ζ_1) or a large system (small μ) of low negative damping (small ζ_1)."

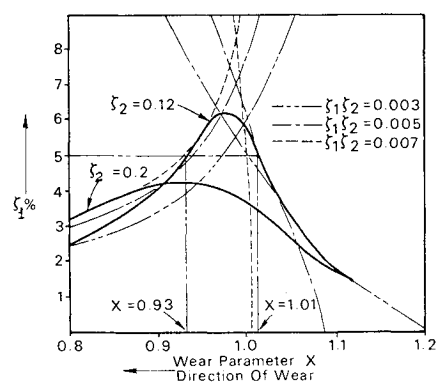

Fig. 5 Stability charts, $\mu = 0.03$ ($\zeta_1 - x$ plots).

Another useful form of stability charts may be obtained by plotting lines of constant ζ_2 in the $\zeta_1 - x$ plane as shown in Fig. 5 for a value of $\mu = 0.03$. The boundaries of constant ζ_2 lines will represent neutral stability of one or both modes, which is the condition when inequalities (21) become equalities. Below each line the two modes are stable and above the line either or both modes will be unstable. The same conclusions may be arrived at, as from Fig. 4, in regard to the effect of increasing ζ_1 or μ on the optimum margin of stability. This, and other conclusions, can best be illustrated by the following example.

Example

The conditions of $\mu = 0.03$, $\zeta_1 = 0.05$, and $\zeta_2 = 0.12$ are shown on both Figs. 4 and 5 to assert that the same margin of stability between $x = 1.01$ and $x = 0.93$ is obtained in both cases. Figure 4 shows that at $\zeta_1 = 0.04$ and a fixed brake frequency ($x = 0.92$), the value of ζ_2 should not exceed 0.22, whereas Fig. 5 shows that at $\zeta_2 = 0.12$ the same damper can handle up to a value of $\zeta_1 = 0.062$ (at $x = 0.98$) for stable operation.

Plotting Method

Since the stability charts represent lines of neutral stability of either or both modes, their equations may be obtained from inequalities (21) at their limiting condition of being equalities. Two equations can thus be obtained,

$$\zeta_1^2 = \zeta_1\zeta_2[r_2^2(x^2 + \mu) - x^2]/(r_2^2 - x^2) \qquad (27)$$

for the upper limit on ζ_1 and

$$\zeta_1^2 = \zeta_1\zeta_2[r_1^2(x^2 + \mu) - x^2]/(r_1^2 - x^2) \qquad (28)$$

for the lower limit on ζ_1. It should be noted that both r_1 and r_2 are functions of the product $\zeta_1\zeta_2$, Eqs. (23) and (24), and thus ζ_1 cannot be separated as an independent variable. However, the upper and lower limits on ζ_1 may be obtained as functions of x and μ for constant values of the product $\zeta_1\zeta_2$. At a given value of μ, constant $\zeta_1\zeta_2$ lines may be plotted in a $\zeta_1 - x$ plane, Fig. 5. If the values of ζ_2 are obtained at each point as $\zeta_2 = \zeta_1\zeta_2/\zeta_1$, constant $\zeta_1\zeta_2$ lines may also be plotted in a $\zeta_2 - x$ plane, Fig. 4. Using the $\zeta_1\zeta_2$ lines in each plane as guidelines, crossings of constant ζ_1 or ζ_2 lines may easily be marked on each $\zeta_1\zeta_2$ line and the stability charts of Figs. 4 and 5 thus obtained. The procedure may then be repeated for different values of μ if they are to be used as design charts for a self-excited two-mass system.

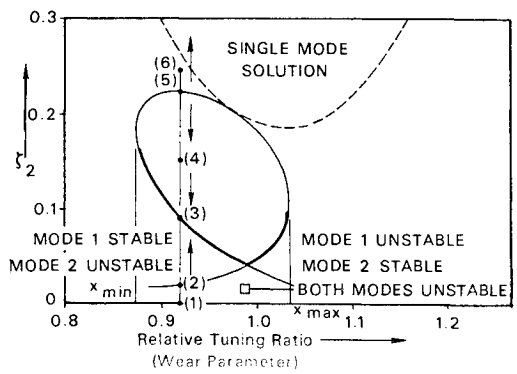

Fig. 6 Neutral stability with velocity-square damping, $\mu = 0.03$, $\zeta_1 = 0.04$. Bold line represents border of neutral stability, arrows give direction of change of ζ_2 from starting condition.

VI. The Condition of Velocity-Square Damping in the Secondary System

The previous discussion has been confined to the condition of having constant viscous damping in the secondary system. The condition of a nonlinear velocity-square damping is of particular interest. In contrast to linear viscous damping the value of ζ_2 is not constant, but an equivalent viscous damping coefficient of varying magnitude may be obtained as outlined in Sec. II. This requires that the secondary system oscillate relative to the primary in order to build up the value of ζ_2 high enough to bring the system to a neutrally stable condition. If the system is tuned at x between x_{max} and x_{min} as shown in Fig. 6 and started from rest, both modes will be unstable and vibration will build up. As the system vibrates, the relative motion between the two masses increases and causes ζ_2 to build up accordingly. The system condition then follows the vertical line marked 1-2-3-4-5 parallel to the ζ_2 axis. At point (2) one mode becomes stable and the other continues to build up. At point (3) the other mode reaches neutral stability and vibration ceases to increase. If the system is started at point (4) both modes will be stable and vibration will die away. This will decrease ζ_2 until point (3) is reached and neutral stability attained. At point (5) the unstable mode continues to be unstable and builds up to the value of ζ_2 for more unstability. The arrows on the figure represent the direction of change of ζ_2 within each region. Stability for velocity-square damping will always mean neutral stability at points along the boundaries of the stability loop. The stability margin M_h will then cover the full range of x within the loop; i.e., $x_{max} - x_{min}$.

This yields to an increase in the available margin of stability over the optimum that can be attained with viscous damping. However, this is counteracted by the fact that only neutral stability can be attained and at least one mode will continue to oscillate at some limiting value in order to attain the proper value of ζ_2 on the boundary of the stability loop.

The variation of the margin of stability M with the amount of negative damping in the system is shown in Fig. 7 for both viscous, M_v, and velocity-square damping, M_h. Those charts can help select the proper mass ratio, or damper size, for any condition of excitation.

VII. Experimental Application

A tuned damper was designed, constructed, and applied to a commercial brake mounted on an actual landing gear and fitted with a lining exhibiting a high vibration level. The following are the design and technical data pertinent to this particular application.

Brake and Lining Data

I_1 = 6.86 lb in. sec^2, ω_1 = 230 cps, ζ_1 = 0.04–0.05 (estimated from torque curve analysis). Normal energy torque = 120,000 in. lb, friction radius = 5.5 in.

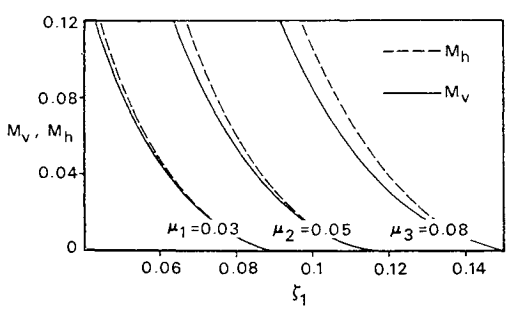

Fig. 7 Stability margin dependence on ζ_1 and μ.

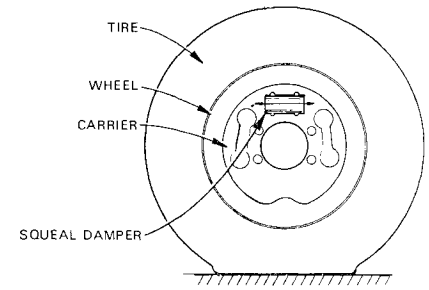

Fig. 8 Damper mounting on brake carrier.

Damper Data

The damper is a linear motion, spring mass system fitted with hydrodynamic, velocity-square damping. I_2 = 0.20 lb in. sec^2 (at 8-in. mounting radius), ω_2 = 220 cps, ζ_2 = 0.1 at 30 g's input vibration level to damper mounting base, μ = 0.03.

The actual mass of the damper accounted for a total increase in the brake weight by 2%, which included the enveloping case of the damper. The inertia ratio μ = 0.03 is different from the mass ratio because the damper is mounted off center as shown in Fig. 8. A specially designed brake carrier, fitted with a patented Bendix Damper† as an integral unit, would result in a net increase of only ½%. This constitutes a considerable weight saving so vital to the aircraft industry.

Tests were conducted at initial rolling speeds of 10, 20, and 30 mph where highest vibration levels were experienced. Except for damper installation and rolling speeds all other influencing factors were not changed during the test.

Cold braking tests were started at an initial temperature of about 150°F and hot tests followed a high-speed normal energy stop. The sequence of testing was the same in both cases, with and without damper, and the brake pressure was adjusted to yield the same deceleration rate.

The angular accelerations were measured by an accelerometer mounted tangentially on the brake. Damper oscillations relative to its mounting case were measured by using a proximity pickup. These measurements indicated that the ratio ζ_2 is in the vicinity of the design value of 0.1, which corresponds to the lower boundaries of the stability loop as predicted by the theory for velocity-square damping conditions, Fig. 6.

The test results are reported in Fig. 9. The vibration acceleration level, in g's, at 5.5-in. radius (location of accelerometer on the brake carrier) is plotted against the initial airplane speed. The design limit on the maximum allowable g-level of 35 g's at damper base corresponds to 25 g's at 5.5-in. radius. Since this limit is set for the response at the highest

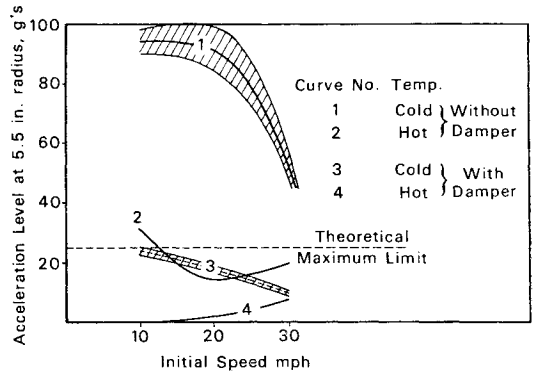

Fig. 9 Experimental vibration levels with and without damper.

† Patent Application No. 652-938; "Damped Vibration Absorber Device," January 31, 1967, A. K. Abu-Akeel and B. W. Anderson, inventors.

excitation level, it is closely approached at 10 mph as expected. At higher speeds the value of ζ_1 is lower and the limit point of stability will correspond to a lower value of ζ_2, and, hence, a lower limit on the g-level. This is clearly demonstrated by the decreasing trend in g-level both with and without damper application.

Further testing is still underway which will help trace the lower boundaries of the stability loop as x changes with progressive brake wear. In this case it is still necessary to repeat the test without the damper to make sure that the excitation level has not changed or to make necessary adjustments in the applicable value of ζ_1.

VIII. Conclusions

The problem of the self-excited two-mass system has been analyzed and a closed-form solution obtained. The conditions of stability of either or both modes have been discussed thoroughly. An outline of the nature of brake excitation is given. Energy method is utilized to treat the possible nonlinear functions introduced in the system. It has been shown that a self-excited two-mass system possesses the property of being stable within a defined range of frequency ratio and secondary system damping. The range of stability is affected by the mass ratio and the negative damping in the system. Reference has been made to the problem when defined by a brake fitted with a tuned damper. The stability charts can then serve as design charts capable of indicating the optimum size, tuning, and damping to be accommodated in a secondary system intended as a damper for a primary brake system. The problem of damping the secondary system by hydraulic (velocity-square damping) rather than viscous means is discussed and the method of utilizing the stability charts outlined. It has been shown that with hydraulic damping the margin of stability is increased but some limiting oscillations of predetermined value have to be allowed within the system. Viscous damping has a smaller range of stability but should damp out any vibration completely; the limiting value in this case is zero amplitude.

The experimental results have confirmed the validity of the theoretical analysis to predict the brake response when fitted with a tuned damper. The brake vibrations were suppressed successfully within the design limits of the damper. The success of this application, without adding an appreciable weight to the brake, represents a long-sought method for control of vibration in brakes. It opens the door for utilizing the harder, more economical linings with the subsequent savings on weight and service cost and increased lining life.

References

[1] Black, R. J., "Evaluation of Brake Lining Materials from Vibration Standpoint, Chatter Tester to Airplane Correlation Methods," Rept. ECD-WV-60-1, unpublished, The Bendix Corp.

[2] Abu-Akeel, A. K., "An Analytical Approach to the Study of Tuned Damper Application to Brake Vibrations," Rept. ECD-WV-67-5, The Bendix Corp.

JAN.-FEB. 1969 J. AIRCRAFT VOL. 6, NO. 1

Jet-Pump Actuation of Variable-Density Subsonic Wind Tunnels

J. C. Gibbings*
University of Liverpool, Liverpool, England

The actuation by jet pumps of variable-density, closed-circuit, subsonic wind tunnels is compared with an existing one-dimensional analysis. The measured performance is correlated in terms of the wind-tunnel power factor. The off-design characteristics of the outlet jet pump under suction conditions are studied, and its performance in combination with the actuator jet pump is given. Two methods of intermittent operation from a storage reservoir are compared.

Nomenclature

a^* = speed of sound for $M = 1$
A = const, Appendix A
A = (with subscript) cross-sectional area
B = const, Appendix A
C = const, Appendix A
C_1,C_2,C_3 = consts, Appendix A
C_f = friction coefficient
C_p = coefficient of specific heat at constant pressure
D = diameter of mixing length
h = specific enthalpy
K = const, Appendix A
L = length of mixing length
m = (with subscript) rate of mass flow
M = (with subscript) Mach number
p = (with subscript) pressure
P = tunnel power factor
R = gas constant
Re = Reynolds number
S = surface area of mixing length
t = tunnel running time
T = (with subscript) temperature
v = (with subscript) velocity
V = reservoir volume
α = const, Appendix A
β = area ratio A_3''/A_3', Appendix A
γ = ratio of the specific heats
η = diffuser efficiency
μ = (with subscripts) mass-flow ratio, secondary to primary flow
ρ = (with subscripts) density
σ = tunnel pressure ratio
ϕ = velocity ratio, Appendix A
ϕ = (with subscripts) nozzle loss coefficient
ϕ_n = friction coefficient, Appendix A
ψ = density ratio, Appendix A

Subscripts

0 = actuator outlet stagnation conditions; also outlet jet pump

Received January 8, 1968; revision received July 22, 1968.

* Lecturer, Department of Mechanical Engineering, Fluid Mechanics Division.